

VAS-Derived Cloud Observations over the Gulf Stream Locale During the Winter Months

R. J. Alliss and S. Raman
Department of Marine, Earth and Atmospheric Sciences
North Carolina State University
Raleigh, NC 27695-8208

Introduction

Clouds have long been recognized as having a major impact on the radiation budget in the earth's climate system. One of the preferred areas for the production of clouds is off the east coast of the United States. The formation of clouds in this region, particularly during the winter months, is caused predominately by the presence of the Gulf Stream, which flows northeastward just off the southeast coast. The geography of the region is such that the cold North American continent lies adjacent to the relatively warm shelf waters (10°C), which in turn are bounded by the much warmer Gulf Stream (25°C). The Sargasso Sea to the east of the Gulf Stream consists of waters slightly cooler than those observed in the Gulf Stream. This unique setup provides the surface forcing necessary for the frequent occurrence of cyclogenesis, coastal frontogenesis, and cold air outbreaks, all of which are major cloud producers. Figure 1, obtained from NOAA-9 Advanced Very High Resolution Radiometer (AVHRR), shows the position and sea surface temperature of the Gulf Stream area on January 28, 1993.

Recently, attempts have been made to characterize the frequency of cloud occurrence and associated cloud properties via inferences from satellite radiance measurements. The CO₂ technique for deriving cloud top pressures (Chahine 1974; Smith et al. 1974) was first applied by Menzel et al. (1983). The technique takes advantage of the differing partial CO₂ absorption in three of the infrared channels, making each channel sensitive to a different level in the atmosphere. Clouds appear in the CO₂ channel images according to their level in the atmosphere. Low clouds will not appear in the high-level

channels, while high clouds appear in all channels. By measuring the upwelling infrared radiation from the earth-atmosphere system in several of the VISSR^(a) Atmospheric Sounder (VAS) CO₂ channels simultaneously, we are able to distinguish thin cirrus clouds due to the transmission of terrestrial radiation through the cirrus.

The objective of this study is to quantitatively evaluate the type and amount of cloudiness most present during the winter months (December-February). The study makes use of 7 years (1985-1993) of multispectral observations using the CO₂ technique from the GOES VAS. Statistics of cloud cover during this period are also presented. Additionally, VAS observations of seven cold air outbreak (CAO) events occurring during January 1993 are presented. Cold air outbreaks are one of the most dynamic events to occur over the Gulf Stream Locale (GSL). This surface energy exchange process occurs when cold dry continental air moves over the warmer Gulf Stream waters, allowing the airmass to destabilize and produce clouds. Since this area is dominated by air-sea interactions such as the CAO, the importance of these processes is essential to understanding cloud genesis.

In the following section of this paper, the methodology and technique for deriving the cloud parameters are described. Current results, including the cloud climatology and cloud distribution during seven cold air outbreak events, are addressed next. The paper concludes with a discussion of future research.

(a) Visible and Infrared Spin-Scan Radiometer.

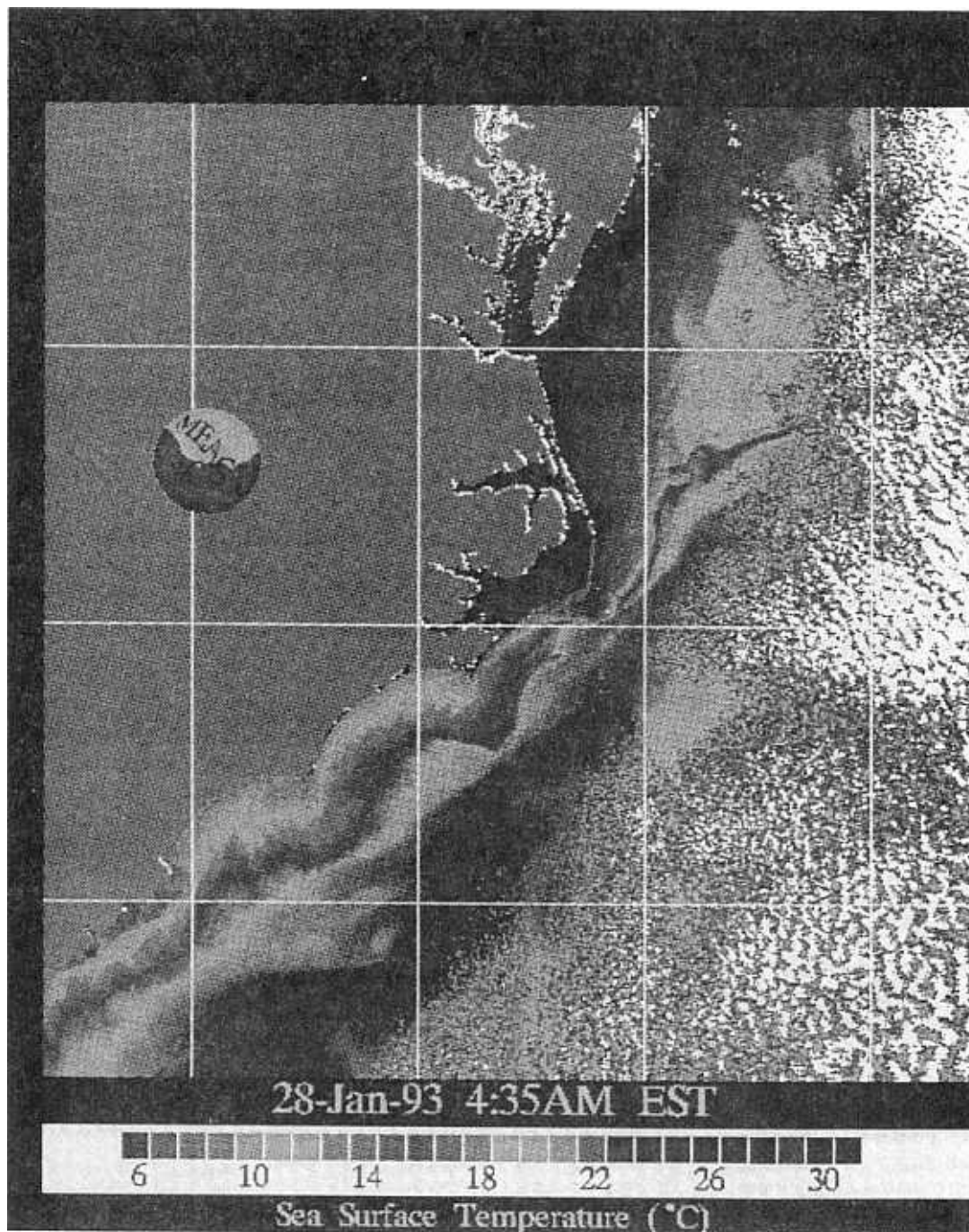


Figure 1. Sea surface temperature of the Gulf Stream Locale obtained from the NOAA9 AVHRR during the cold air outbreak of 28 Jan. 93.

Methodology and Description of CO₂ Technique

The VAS radiometer detects infrared radiation in 12 spectral bands that lie between 3.9 and 15 μm with 7- or 14-km resolution. The 15-μm CO₂ band channels provide good sensitivity to the temperature of relatively cold regions of the atmosphere. An example of the vertical resolution of the three CO₂ channels used in this study is given by the temperature profile weighting functions shown in Figure 2. Each curve in the figure shows the sensitivity to variations in atmospheric temperature of the radiance observed by the indicated channel. Only clouds above the 350-mb level contribute significantly to the radiance to space observed by the 14.2-μm band (channel 3), while the 14.0-μm band (channel 4) senses down to 700 mb and the 13.3-μm band (channel 5) senses down near the surface of the earth.

To assign a cloud top pressure to a given cloud element, the CO₂ technique is used. As shown by Smith and Platt

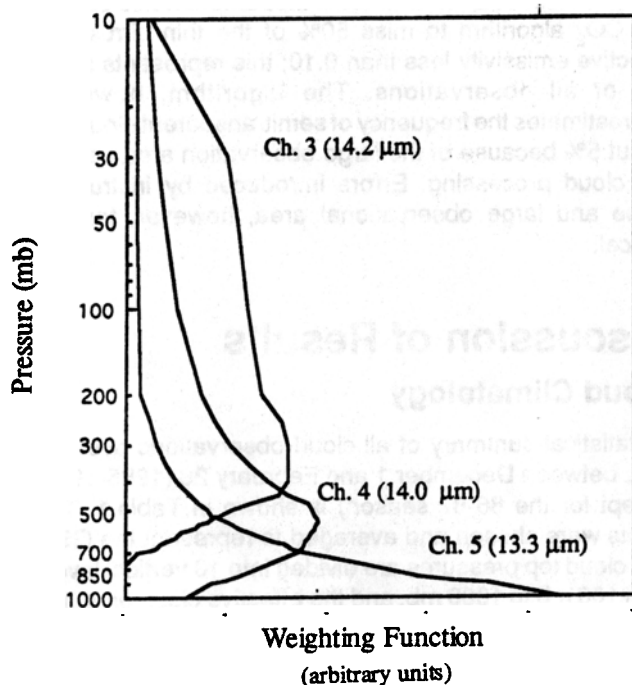


Figure 2. The temperature profile weighting function for the VAS CO₂ spectral bands centered at 14.2, 14.0 and 13.3 μm.

(1978), the ratio of the deviations in cloud-produced radiances, $I(v)$, and the corresponding clear air radiances, $I_{cl}(v)$, for two spectral channels of frequency v_1 and v_2 viewing the same field-of-view can be written as

$$\frac{I(v_1) - I_{cl}(v_1)}{I(v_2) - I_{cl}(v_2)} = \frac{\epsilon_1 \int_{P_s}^{P_c} \tau(v_1, p) \frac{dB[v_1, T(p)]}{dp} dp}{\epsilon_2 \int_{P_s}^{P_c} \tau(v_2, p) \frac{dB[v_2, T(p)]}{dp} dp} \quad (1)$$

- where ϵ = the cloud emissivity
- P_s = the surface pressure
- P_c = the cloud pressure
- $\tau(v, p)$ = the fractional transmittance of radiation of frequency v emitted from the atmospheric pressure level (p) arriving at the top of the atmosphere ($p=0$)
- $B[v, T(p)]$ = the Planck radiance of frequency v for temperature $T(p)$.

If the frequencies are close together, then ϵ_1 approximates ϵ_2 , and one has an expression by which the pressure of the cloud within the field-of-view (FOV) can be specified.

The left side of Equation (1) is inferred from the observed radiances from VAS in a given FOV, and the clear air radiances are inferred from spatial analyses of VAS clear radiance observations in neighboring FOVs. The right side of Equation (1) is calculated from a temperature profile and the profiles of atmospheric transmittance for the spectral channels as a function of P_c , the cloud top pressure (1000 to 100 mb is spanned by discrete values at 50-mb intervals). Global analyses of temperature and moisture profiles from the National Meteorological Center (NMC) are used.

The optimum cloud top pressure is found when the absolute difference of the left side (v_1, v_2) minus the right side (v_1, v_2, P_c) is a minimum. Using the ratios of radiances of the three CO₂ spectral channels, three separate cloud top pressures can be determined (14.2/14.0, 14.0/13.3, and 14.2/13.3). If $(I - I_{cl})$ is within the noise response of the instrument (roughly 1 mW/m²/st/cm⁻¹), the resulting P_c is rejected. As described by Menzel et al. (1983), the most representative cloud height and amount are those that best satisfy the radiative transfer equation for the three CO₂ channels.

Once cloud top pressure and height have been determined, an effective cloud amount (also referred to as effective

emissivity) can be evaluated from the infrared window channel data using the following relation:

$$N \varepsilon = \frac{I(w) - I_{c1}(w)}{B[w, T(P_c)] - I_{c1}(w)} \quad (2)$$

The effective cloud amount is the ratio of the radiance difference the observed cloud produces to the radiance difference an opaque cloud at the same level would produce in the infrared window. Here

N = the fractional cloud cover within the FOV
 $N\varepsilon$ = the effective cloud amount
 w = the window channel frequency
 $B[w, T(P_c)]$ = the opaque cloud radiance.

Using the infrared window channel and the three cloud top pressures, three effective cloud amount determinations are made.

If no ratio of radiances can be reliably calculated because $I - I_{c1}$ is within the instrument noise level, then a cloud top pressure is calculated directly from the VAS-observed 11.2 μm infrared-window channel brightness temperature comparison with the temperature profile, and the effective emissivity is assumed to be unity. This occurs for most low clouds below 700 mb; here, the CO_2 technique cannot find a pair of weighting functions where both have adequate sensitivity. Thus, all clouds are assigned a cloud top pressure either by the CO_2 ratios or the infrared window calculations.

Fields of view are determined to be clear or cloudy through inspection of the 11.2 μm brightness temperature with a correction for moisture absorption. If the moisture-corrected 11.2 μm brightness temperature is within 2 K of the known surface temperature (taken from the 1000 mb NMC model analysis adjusted with hourly observations), then the FOV is assumed to be clear and no cloud parameters are calculated.

The VAS CO_2 technique is independent of the fractional cloud cover. Cloud heights and effective cloud emissivities can be determined for partially cloudy FOVs. However, there are a few assumptions. The effective cloud emissivity is assumed to be independent of wavelength. The cloud is assumed to be of infinitesimal thickness; Smith and Platt (1978) have indicated that this assumption introduces errors approaching one-half (one-quarter) the thickness of

the cloud for optically thin (thick) clouds where the integrated emittance is less than (greater) 0.6.

The CO_2 algorithm determines the height of the radiative center of the cloud. For optically thick clouds, this is near the cloud top; for optically thin clouds, it is near the cloud middle.

The VAS CO_2 technique assumes the presence of only one cloud layer; when multiple layers are sensed, it derives a cloud altitude in between the altitudes of the two separate layers. Multilayer cloud situations where an opaque cloud underlies a transmissive cloud cause errors of about 100 mb in the height of the transmissive cloud; for most cases the cloud is found to be too low in the atmosphere. The error in transmissive cloud height is largest when the underlying opaque layer is in the middle troposphere (400 - 700 mb) and small to negligible when the opaque layer is near the surface or close to the transmissive layer.

Because the VAS FOV resolution is coarse (7 km), very small element clouds are difficult to detect. Also, because the weighting functions for the VAS channels are broad, the vertical resolution is limited. Instrument noise causes the CO_2 algorithm to miss 50% of the thin cirrus with effective emissivity less than 0.10; this represents about 5% of all observations. The algorithm, however, overestimates the frequency of semitransparent clouds by about 5% because of the large observation area used in the cloud processing. Errors introduced by instrument noise and large observational area, however, tend to cancel.

Discussion of Results

Cloud Climatology

A statistical summary of all cloud observations over the GSL between December 1 and February 28 (1985-1993, except for the 86-87 season) is shown in Table 1. Ten points were chosen and averaged to represent the GSL. The cloud top pressures are divided into 10 vertical levels from 100 mb to 1000 mb, and the effective cloud amounts are subdivided into five intervals from 0 to 1.0.

As indicated in the preceding section, the effective cloud amount is defined as the product of the fractional cloud cover N and the emissivity of the cloud ε for each

Table 1. Cloud statistics (%) for the Gulf Stream Locale during the 7 winters (Dec. - Feb.) between 1985 and 1993, not including 1986-1987.

Level (mb)	Effective Emissivity (%)				
	0.0 - 0.2	0.2 - 0.4	0.4 - 0.6	0.6 - 0.95	0.95 - 1.0
100-199	0.0	0.0	0.0	0.0	0.2
200-299	1.1	2.6	1.9	6.1	3.2
300-399	0.5	2.3	2.9	7.8	2.7
400-499	0.1	0.8	1.5	3.0	2.1
500-599	0.0	0.1	0.3	0.9	2.3
600-699	0.0	0.0	0.0	0.1	7.4
700-799	0.0	0.0	0.0	0.0	6.8
800-899	0.0	0.0	0.0	0.0	6.9
900-999	0.0	0.0	0.0	0.0	5.4
1000	30.9	0.0	0.0	0.0	0.0

30.9 % clear

32 % cirrus

37% opaque

observational area. When N_e is less than unity, VAS may be observing broken opaque cloud, overcast transmissive cloud, or broken transmissive cloud. All of these possibilities are labeled as "cirrus." It is not possible to distinguish between them with the CO_2 technique. Here "cirrus" refers to an observation where the VAS radiometer detects radiation both above and below a cloud layer.

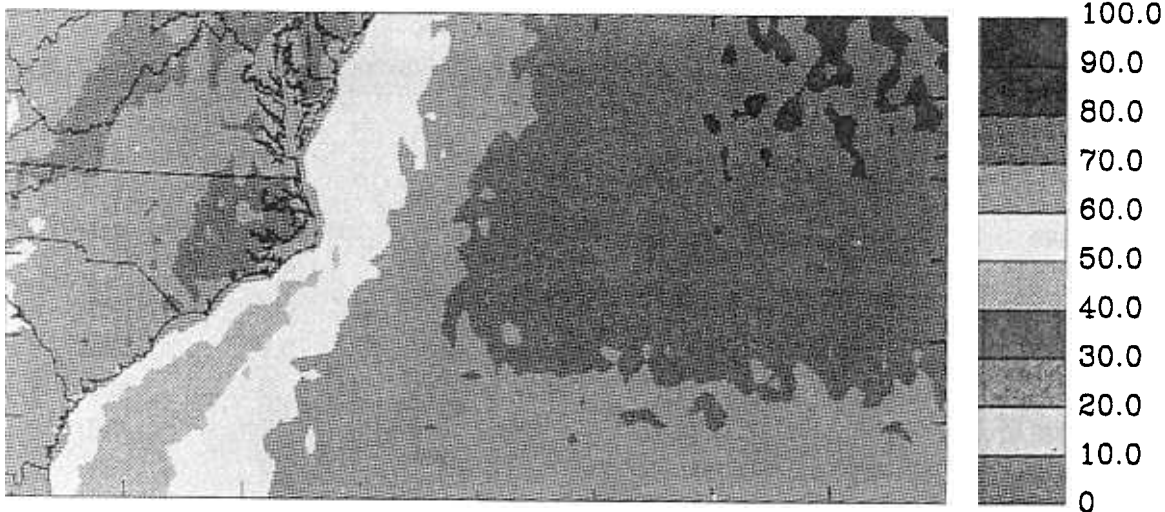
Effective emissivity observations less than 0.95 are labeled as cirrus ranging from the thin low emissivity clouds on the left to the thick high emissivity clouds on the right. Those greater than 0.95 are considered to be opaque clouds, since the cloud top height derived from Equation (1) is very close to the height derived from the window channel by itself. Most cloud heights below 700 mb were determined from the infrared window channel and, thus, were assumed to have an effective emissivity of 1. This assumption prevents the misinterpretation of low broken cloud as cirrus.

Table 1 reveals that clouds were detected on average 69% of the time during this period, with 32% of those observations identified as cirrus and 37% identified as opaque cloud. Independent observations by Warren et al. (1986) found

that the GSL is covered by clouds over 70% of the time. Cirrus observations ranged from 100 to 600 mb and varied in thickness. Opaque clouds were detected at all levels but most commonly found between 600 and 850 mb. High clouds ($P_c < 400$ mb) were observed 31% of the time, while clouds between 400 and 700 mb were observed 19% of the time. Low clouds having cloud top pressures no less than 700 mb were found approximately 19% of the time. Clear sky observations were found on average nearly 33% of the time during the winter months.

Figure 3 shows the geographical distribution of percent cloud amount (or effective emissivity) and frequency of clear sky during the same period. The area covered by this region is from 30° to 40°N latitude and 60° to 85°W longitude. During this seven-year climatology, clouds occurred most frequently east of the Gulf Stream region (70%) and consisted mainly of opaque clouds ranging in height from 800 mb to 400 mb. Over the axis of the Gulf Stream, cloudiness was detected no more than 50% of the time, consisting mainly of high transparent clouds. In the lower panel, VAS observations where the CO_2 technique derives a cloud top pressure of 1000 mb are shown. These

PERCENT CLOUD AMOUNT
Nov 30 1985 to Mar 1 1993 99 UTC



FREQUENCY OF CLEAR SKY
Nov 30 1985 to Mar 1 1993 99 UTC

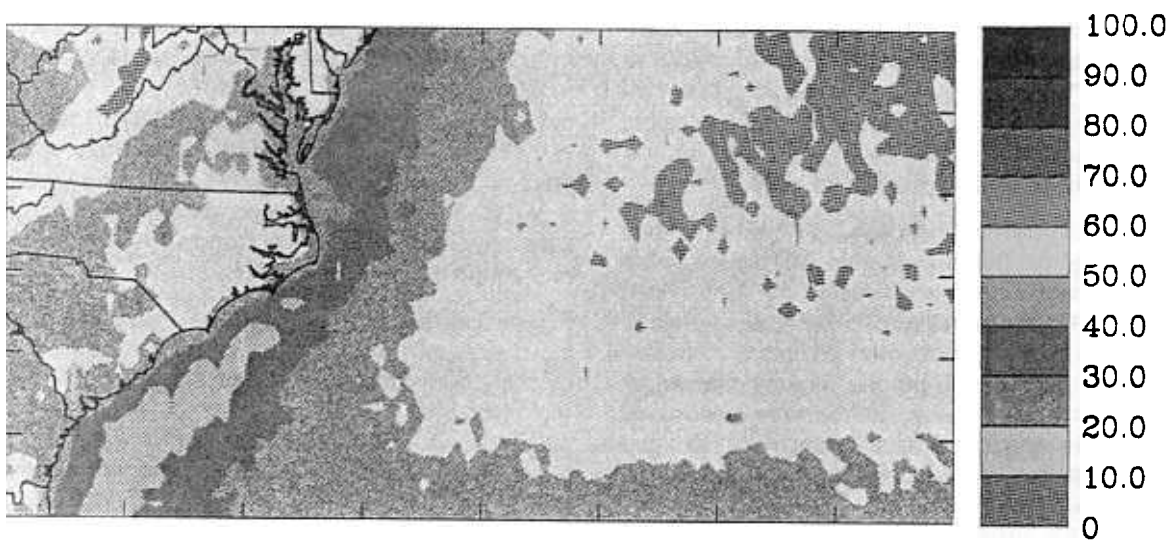


Figure 3. Percent cloud amount and frequency of clear sky during the winter months (Dec.-Feb.) 1985-1993, not including 1986-1987.

observations are labeled as clear sky. Clear sky conditions were found most often along the axis of the Gulf Stream with a marked decrease to the east.

Cloud Generation Processes Associated with CAOs

About 15 to 20 CAO events affect the mid-Atlantic region annually between December and March, with about five of those being intense (air temperature $< 0^{\circ}\text{C}$) (Grossman 1988). During January 1993, seven CAO events occurred, with the most intense observed on January 28.

Figure 4 is a visible image from GOES-7 at 17 UTC 4 Jan 93. Cloud streets are observed east of the GSL. During the seven CAOs, VAS clear sky observations over the GSL were observed nearly 50% of the time. Compared with the climatology, clear sky observations during these CAOs were found nearly 20% more often; however, high thin cirrus clouds were observed much less frequently (18%). Low opaque clouds were observed 19% of the time, about the same frequency as the climatology. Figure 5 shows the percent cloud amount and frequency of clear sky during the seven CAO events. The 25% of cloudiness observed over the Gulf Stream to the east of Cape Hatteras is in response to the sharp gradient in sea surface temperature (SST) in the region.

During CAOs, cold dry airmass is modified as it moves across the shelf waters. Over this region the air is not saturated, thus cloud genesis is inhibited. Depending on the air temperature, the trajectory and intensity of the wind, clouds typically develop on the eastern side of the Gulf Stream where the airmass has become most unstable. This conditioning period is most responsible for the cloud minimum seen over the GSL (Figure 4). The SST image shown in Figure 1 shows this process. No clouds are observed over the shelf waters and the western Gulf Stream, as indicated by the unobstructed view of the sea surface. However, on the eastern side of the Gulf Stream, the SST field becomes obscured as attenuation due to low clouds increases. The attenuation effects become more dominant further offshore. Over the Sargasso Sea, to the east of the Gulf Stream, low clouds were identified 36% of

the time, approximately 10% more than in the climatology. These consisted of cumulus and stratocumulus which developed in the boundary layer as the cloud top pressures were estimated to be around 900 mb.

The other 24 days of the month were characterized by an above-normal amount of cloudiness. The winds in the region were predominately from the southwest, transporting warm moist air from the Gulf of Mexico northeastward. Clouds were observed approximately 70% of the time over the GSL and over the entire domain. Of the 70% of cloud observations, 50% were identified by VAS as cirrus cloud. VAS clear sky observations were observed only 5% to 10% of the time.

Conclusions and Future Work

The principal finding is that the occurrence of clouds over the Gulf Stream Locale during the winter months is dependent on atmospheric processes and their likely interaction with the Gulf Stream. A cloud climatology consisting of seven winters indicates that clouds occur approximately 70% of the time. However, during periods of cold air outbreaks, cloudiness occurs much less frequently. From the limited number of analyzed CAO events, VAS observations indicate that the Gulf Stream Locale plays an important role in the formation and maintenance of clouds, particularly shallow, opaque clouds downwind of the Gulf Stream Locale.

Future work will focus on isolating other atmospheric processes and their relationship to cloud production over the Gulf Stream Locale. In addition, diurnal effects of cloud distribution and the land, air-sea interaction process will be investigated and reported on in the future.

Acknowledgments

This work was supported by the U.S. Department of Energy Atmospheric Radiation Measurement Program under contract 091575-A-Q1 with Pacific Northwest Laboratory.

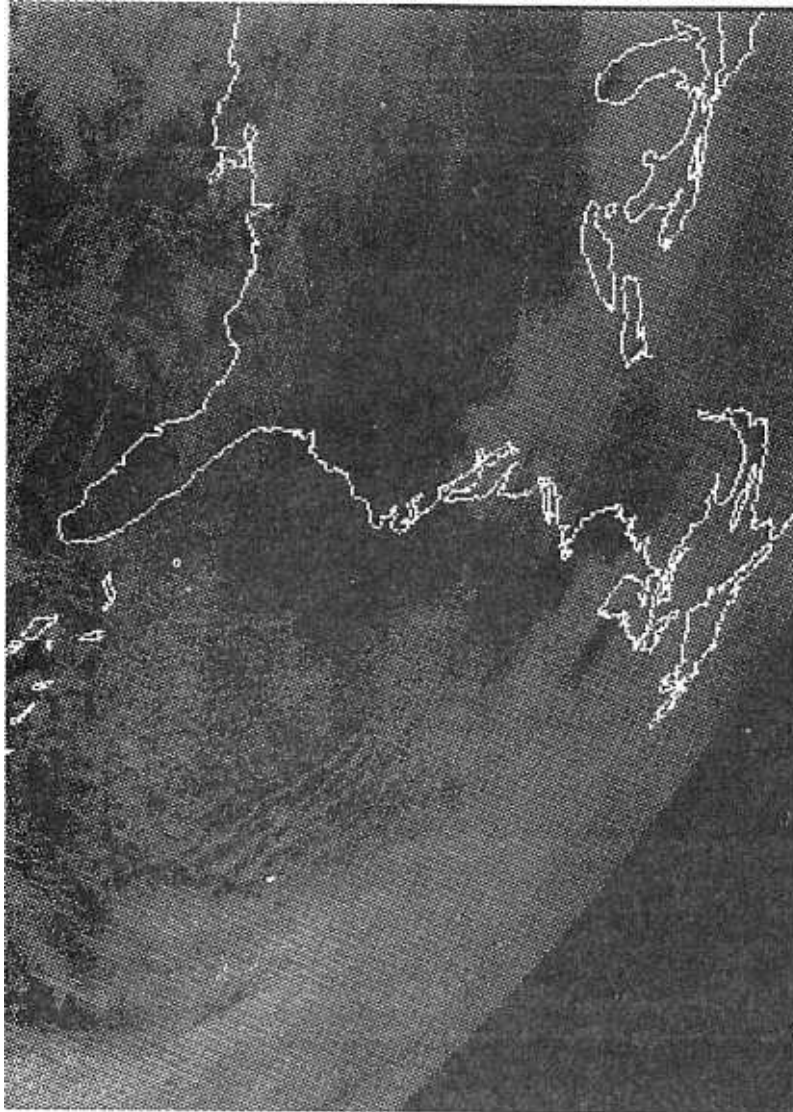
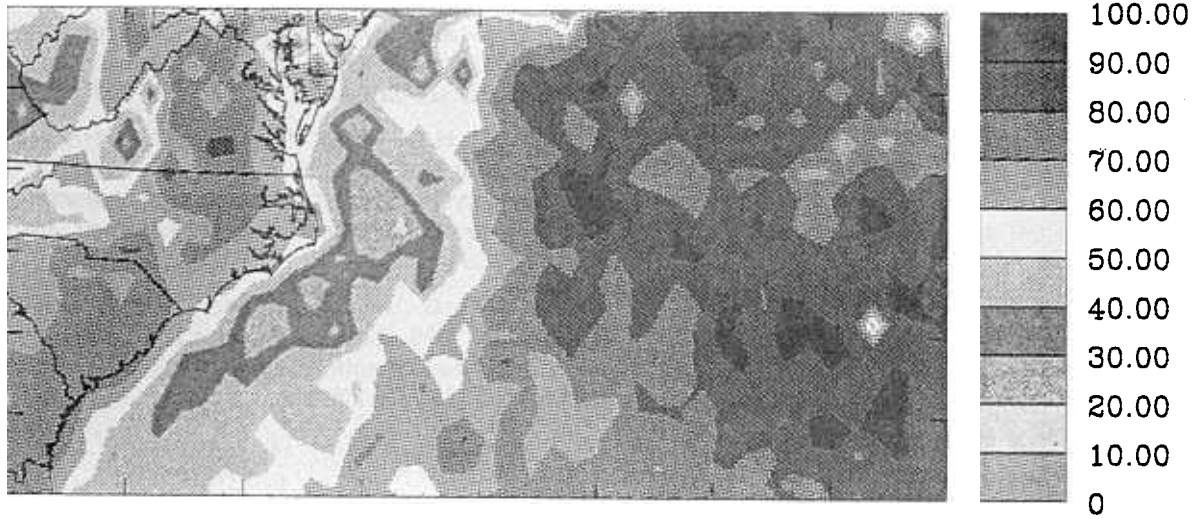


Figure 4. GOES-7 visible imagery (17 UTC) during the CAO event on 28 Jan. 1993. Cloud streets are readily visible as the cold dry continental air moves over the warmer Gulf Stream.

PERCENT CLOUD AMOUNT



FREQUENCY OF CLEAR SKY

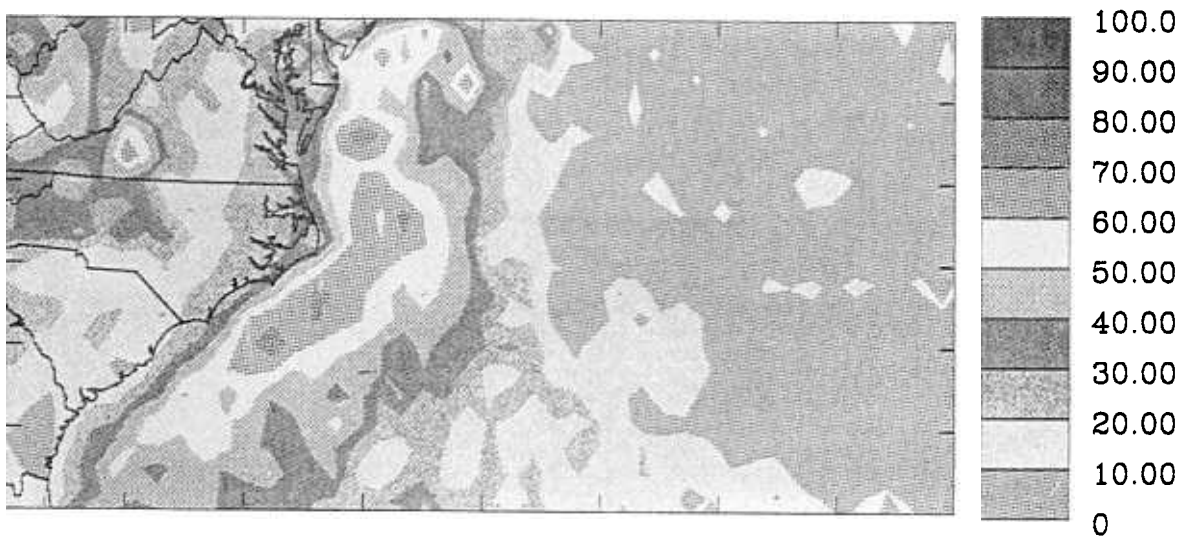


Figure 5. Percent cloud amount and frequency of clear sky during seven cold air outbreak events, January 1993.

References

- Chahine, M. T. 1974. Remote sounding of cloudy atmospheres. 1: The single cloud layer. *J. Atmos. Sci.* **31**:233-243.
- Grossman, R. L. 1988. Boundary Layer Warming by Condensation: Air sea interaction during an extreme cold air outbreak from the eastern coast of the United States. *Proceedings, Seventh Conference on Ocean-Atmosphere Interaction*. American Meteorological Society, Boston, Massachusetts.
- Gruber, A., and T. S. Chen. 1988. Diurnal variation of outgoing longwave radiation. *J. Clim. Appl. Meteorol.* **8**:1-16.
- Menzel, W. P., W. L. Smith, and T. R. Stewart. 1983. Improved cloud motion wind vector and altitude assignment using VAS. *J. Clim. Appl. Meteorol.* **22**:377-384.
- Rossow, W. B., and A. A. Lacis. 1990. Global, seasonal cloud variations from satellite radiance measurements. Part II: Cloud properties and radiative effects. *J. Clim.* **3**:1204-1253.
- Smith, W. L., and C.M.R. Platt. 1978. Intercomparison of radiosonde, ground based laser, and satellite deduced cloud heights. *J. Appl. Meteorol.* **17**:1796-1802.
- Smith, W. L., H. M. Woolf, P. G. Abel, C. M. Hayden, M. Chalfant, and N. Grody. 1974. Nimbus 5 sounder data processing system. Part 1: Measurement characteristics and data reduction procedures. NOAA Tech. Memo., NESS 57, 99 pp.
- Warren, S. G., C. J. Hahn, J. London, R. M. Chervin, and R. L. Jenne. 1986. Global distribution of total cloud cover and cloud type amounts over land. NCAR Tech. Note NCAR/TN-273+STR, 228 pp.